Journal of
Materials Chemistry

Cite this: *J. Mater. Chem.*, 2011, **21**, 13554

www.rsc.org/materials

PAPER

Tetraphenylethylene-based fluorescent porous organic polymers: preparation, gas sorption properties and photoluminescence properties†

Qi Chen,[a] Jin-Xiang Wang,[ab] Fen Yang,[ab] Ding Zhou,[a] Ning Bian,[a] Xin-Jian Zhang,[a] Chao-Guo Yan[b] and Bao-Hang Han*[a]

Received 23rd April 2011, Accepted 1st July 2011
DOI: 10.1039/c1jm11787d

Tetraphenylethylene-based porous organic polymers were synthesized efficiently through a Suzuki coupling polycondensation or oxidative coupling polymerization. According to the obtained nitrogen physisorption isotherms, the Brunauer–Emmett–Teller specific surface area values for these porous materials vary between 472 and 810 $m^2 g^{-1}$. Using the same linker monomer, the specific surface area of copolymer materials (TPOP-3 or TPOP-5) prepared by two different core structural monomers (tetraphenylethylene and spirobifluorene) is higher than those of the respective homopolymers. Gravimetric hydrogen adsorption isotherms show that the adsorption capacity for hydrogen is up to 1.07 wt% at 1.13 bar and 77 K. Furthermore, incorporation of tetraphenylethylene moieties into these polymers can induce high photoluminescence (λ_{max}: 530–610 nm) in the solid state. Thanks to the propeller-like structure and aggregation-induced emission characteristics, tetraphenylethylene is to be a promising building block for designing porous polymers with special properties.

1. Introduction

Porous organic polymers (POPs), exhibiting potential applications in heterogeneous catalysis[1] and gas storage,[2] can be categorized into several classes, such as hyper-crosslinked polymers (HCPs),[3] polymers of intrinsic microporosity (PIMs),[4] covalent organic frameworks (COFs),[5] and conjugated microporous polymers (CMPs).[6] Most of the porous organic polymers possess intrinsic properties of large surface areas, high chemical stabilities, and low skeletal density,[7] which have drawn great interests of scientists in recent years.

By selecting the proper chemical reactions or various building blocks, versatile porous polymers can be obtained efficiently, which show high flexibility in the molecular design. For example, palladium-catalyzed Sonogashira–Hagihara coupling reaction[6] and oxidative coupling of thiophenes[8] were used for preparation of poly(aryleneethynylene) CMPs and poly(arylenethiophene) CMPs, respectively. Nickel-promoted Yamamoto polymerization was used as a novel route to synthesize microporous polymer materials,[9] in which the polymerization can be performed with only a single monomer. Dioxane formation by polyphenols and tetrafluoroarylenes was designed for synthesis of a wide variety of PIMs.[4] Some microporous polymers have been prepared by reactions involving triazine formation[10] from aromatic nitriles or alkyne trimerization.[7,8a] Meanwhile, using rigid or contorted building blocks as the cores of polymers often plays an important role in designing porous materials with high surface areas. It has been proved that microporous organic polymers containing spirocyclic units,[11,8a] tetrahedral carbon- and silicon-centred monomers[12] usually possess large surface area (greater than 700 $m^2 g^{-1}$). Recently, the cubic siloxane-cages[13] and bulky adamantane[14] structures have also been used in preparation of porous polymers. The monomer structures show a significant influence on the surface property and porous structure of porous polymers. Cooper and coworkers[6b] have demonstrated the feasibility of systematically controlling the strategy of fine-tuning the average micropore size and surface area by copolymerization of monomers with different strut lengths.

Since Tang's group reported the aggregation-induced emission (AIE) features of tetraphenylethylene-based luminophors,[15] tetraphenylethylene (TPE)-based AIE active materials have already shown practical applications in OLEDs,[15] chemo-sensors,[16] and bio-probes,[17] owing to their enhanced emission in the aggregate form or solid state. The AIE effect can greatly improve the fluorescence quantum yields of the molecules by up to three orders of magnitude, enhancing the photoluminescence intensity

---

[a] *National Center for Nanoscience and Technology, Beijing, 100190, China. E-mail: hanbh@nanoctr.cn; Fax: +86-10-82545576*
[b] *College of Chemistry & Chemical Engineering, Yangzhou University, Yangzhou, 225002, China*

† Electronic supplementary information (ESI) available: TGA data of TPOPs; ^{13}C CP/MAS NMR spectra of TPOP-4 and TPOP-5; nitrogen adsorption–desorption isotherms of TPOP-2 and TPOP-3; BET specific surface areas of TPOPs calculated over different relative pressure ranges and corresponding BET specific surface area plots; logarithmic plots of nitrogen adsorption isotherms and hydrogen adsorption isotherms of TPOPs measured at 77 K; SEM images of TPOP-1 and TPOP-2; photos of TPOPs under UV light (365 nm) illumination; ^{1}H NMR and ^{13}C NMR of **M-4**. See DOI: 10.1039/c1jm11787d

from faint luminophores into strong emitters.[16a] The steric effect of the peripheral phenyl rings can prevent TPE from packing *via* π–π stacking interactions.[15] Therefore, TPE molecules exhibit propeller-like, nonplanar conformation, which are different from the contorted spiro-cyclic compounds and the planar π-system molecules. Thanks to its efficient preparation, propeller-like structure, and AIE characteristics, tetraphenylethylene is expected to be a novel building block for the design of porous polymers with special properties. Herein, preparation and properties of TPE-based porous organic polymers (TPOPs) are reported for the first time. The polymer synthesis was facilitated smoothly by Suzuki coupling polycondensation or oxidative coupling polymerization. The BET specific surface area data for these polymers vary between 472 and 810 m^2 g^{-1}. Gravimetric hydrogen adsorption isotherms show that the hydrogen uptake of the synthetic porous polymer is up to 1.07 wt% at 1.13 bar and 77 K. Incorporation of TPE moieties into these polymers induces high photoluminescence (λ_{max}: 530–610 nm) in the solid state.

2. Experimental section

2.1. Materials and characterization

All chemical reagents were commercially available and used as received unless otherwise stated. Benzene-1,4-diboronic acid (BDBA) and tetrakis(triphenylphosphine)palladium(0) were purchased from Acros. Tetrakis(4-bromophenyl) ethylene (**M-1**),[18] 2,2′,7,7′-tetrabromo-9,9′-spirobifluorene (**M-2**),[19] tetrakis(4-bromophenyl) methane (**M-3**),[20] and 2,2′,7,7′-tetrakis(2-thienyl)-9,9′-spirobifluorene (**M-5**)[8] were prepared according to reported methods, respectively.

The ^1H and ^{13}C NMR spectra were recorded on a Bruker DMX400 NMR spectrometer. Solid state cross-polarization magic angle spinning (CP/MAS) NMR was recorded on a Bruker Avance III 400 NMR spectrometer. Nitrogen sorption isotherms were obtained with a Micromeritics ASAP 2020M + C accelerated surface area and porosimetry analyzer at 77 K. The samples were degassed overnight at 120 °C. The obtained adsorption–desorption isotherms were evaluated to give the pore parameters, including Brunauer–Emmett–Teller (BET) specific surface area, pore size, and pore volume. The pore size distribution was calculated from the adsorption branch with the nonlocal density function theory (NLDFT) approach. SEM observations were carried out using a Hitachi S-4800 microscope (Hitachi Ltd., Japan) at an accelerating voltage of 6.0 kV and equipped with a Horiba energy dispersive X-ray spectrometer. TEM observations were carried out using a Tecnai G^2 20 S-TWIN microscope (FEI, USA) at an accelerating voltage of 200 kV. The fluorescence spectra were measured using a Perkin-Elmer LS55 luminescence spectrometer. X-Ray diffraction (XRD) patterns of the samples were acquired from 0.5 to 35° by a Philips X'Pert PRO X-ray diffraction instrument. Thermogravimetric analyses (TGA) were performed on a Pyris Diamond thermogravimetric/differential thermal analyzer by heating the samples at 10 °C min^{-1} to 800 °C in the atmosphere of nitrogen.

2.2. Synthesis of tetrakis(2-thienyl) ethylene (M-4)

To the solution of tetrakis(4-bromophenyl)ethylene (400 mg, 0.617 mmol) and 2-thiopheneboronic acid (395 mg, 3.086 mmol) in 30 mL of THF was added a 10 mL saturated solution of potassium carbonate, and then degassed by bubbling nitrogen gas for 15 min. After adding $Pd(PPh_3)_2Cl_2$ (60 mg, 0.085 mmol) under nitrogen protection, the reaction mixture was refluxed for 48 h and then cooled down to room temperature. The resulting mixture was extracted with ethyl acetate three times. The combined organic layer was washed with deionized water and dried over sodium sulfate. After concentration under reduced pressure, the remaining oil was purified by column chromatography using *n*-hexane–chloroform (5 : 1) as eluent to give the desired product **M-4** (223 mg, 55%) as a light yellow solid. ^1H NMR (400 MHz, $CDCl_3$): δ 7.40 (d, *J* = 8.4 Hz, 8H, Ar–*H*), 7.27 (d, *J* = 3.6 Hz, 4H, Th–*H*), 7.23 (dd, *J* = 4.8 Hz, 0.8 Hz, 4H, Th–*H*), 7.09 (d, *J* = 8.4 Hz, 8H, Ar–*H*), 7.04 (dd, *J* = 5.2 Hz, 3.6 Hz, 4H, Th–*H*). ^{13}C NMR (100 MHz, $CDCl_3$): δ 144.3, 142.9, 140.4, 132.8, 132.1, 128.1, 125.3, 124.8, 123.2.

2.3. Synthesis of TPOPs by Suzuki coupling polymerization

TPOP-1, TPOP-2, and TPOP-3 were synthesized by palladium-catalyzed Suzuki coupling condensation between BDBA and arylbromide. A representative preparation for TPOP-3 is given in detail as follows.

A mixture of tetrakis(4-bromophenyl) ethylene (162 mg, 0.25 mmol), 2,2′,7,7′-tetrabromo-9,9′-spirobifluorene (158 mg, 0.25 mmol), and BDBA (163 mg, 1.0 mmol) in dimethylformamide (DMF, 100 mL) was degassed by the freeze–pump–thaw cycles. To the mixture was added an aqueous solution of potassium carbonate (2.0 M, 16 mL) and tetrakis(triphenylphosphine)palladium(0) (50 mg, 55 μmol). The resulting solution was degassed and purged with nitrogen, and stirred at 150 °C for 36 h. The mixture was cooled to room temperature and poured into water. The insoluble precipitate was filtered and washed with water, methanol, and acetone to remove any unreacted monomers or catalyst residues. Further purification of the polymer was carried out by Soxhlet extraction with water, methanol, and tetrahydrofuran (THF) for 24 h, respectively, to give TPOP-3 (240 mg) as a solid.

When 2,2′,7,7′-tetrabromo-9,9′-spirobifluorene was replaced by the same equivalent of tetrakis(4-bromophenyl) methane, TPOP-2 can be obtained according to the procedure as described above. As for TPOP-1, only tetrakis(4-bromophenyl) ethylene was used as core structural monomer and its amount is a half equivalent of BDBA.

2.4. Synthesis of TPOPs by oxidative coupling polymerization

TPOP-4 and TPOP-5 were synthesized through oxidative coupling polymerization promoted by anhydrous $FeCl_3$. A representative preparation for TPOP-5 is given in detail as follows.

To the solution of tetrakis(2-thienyl) ethylene (90 mg, 0.093 mmol) and 2,2′,7,7′-tetrakis(2-thienyl)-9,9′-spirobifluorene (90 mg, 0.095 mmol) in 50 mL of anhydrous $CHCl_3$ was added anhydrous $FeCl_3$ (440 mg, 2.72 mmol). The solution mixture was stirred at room temperature for 2 d under nitrogen protection, and then 100 mL of methanol was added to the above reaction mixture. The resulting mixture was kept stirring for another hour and the precipitate was collected by filtration. After washed with methanol, the obtained solid was stirred vigorously in 37% HCl solution for 2 h. The suspension was then filtered and washed with water and methanol. After extraction in a Soxhlet extractor with methanol for 24 h, and then with THF for another 24 h, the desired polymer was collected (81% in yield) and dried in a vacuum oven at 110 °C overnight.

When only tetrakis(2-thienyl) ethylene was used as the core structural monomer, TPOP-4 was obtained according to the procedure as described above in a yield of 77%.

3. Results and discussion

2,2′,7,7′-Tetrabromo-9,9′-spirobifluorene and tetrakis(4-bromophenyl) methane, as two types of monomers with spiral and tetrahedral core structures, have been commonly selected for constructing intrinsic porosity within the polymers by several groups.[12] In this work, tetrakis(4-bromophenyl) ethylene was first used as one of the non-planar building blocks for preparation of porous polymers, owing to its propeller-like structure and AIE characteristics. It can be obtained quantitatively from 4,4′-dibromobenzophenone through a titanium(0)-catalyzed McMurry reaction.[18] As shown in Scheme 1, the porous homopolymers TPOP-1 and TPOP-4 were synthesized efficiently by a Suzuki coupling polycondensation and oxidative coupling polymerization promoted by anhydrous $FeCl_3$, respectively. Considering that the different types of contorted or non-planar core structures with similar reactivities would have different impact on the surface areas of polymers, three copolymers (TPOP-2, TPOP-3, and TPOP-5) containing two different types of core structures were also prepared using the same methods.

All the polymers are chemically stable even when exposed to dilute solutions of acid and base, such as HCl and NaOH. Thermal analysis (Fig. S1†) shows that the material is stable up to 300 °C in all cases under nitrogen and there has been no evidence for distinct glass transition for these polymers below the thermal decomposition temperature due to the nature of their cross-linking structures, which is consistent with good physicochemical robustness for most of the porous organic polymers.[21] In order to confirm their structures, all polymers were characterized at the molecular level by ^{13}C CP/MAS NMR spectroscopy. The ^{13}C NMR spectra for the porous polymers with assignment of the resonances are shown in Fig. 1. For polymers TPOP-1, TPOP-2, and TPOP-3 prepared by Suzuki coupling polymerization, there are two broad peaks approximately at 140 and 127 ppm, which are assigned to the substituted vinyl and phenyl carbons (140 ppm) and the unsubstituted phenyl carbons (127 ppm), respectively. As to TPOP-2, there are two other peaks at 146.1 and 64.9 ppm corresponding to substituted phenyl carbons and quaternary carbons in tetraphenylmethane moieties, respectively. For TPOP-3, besides the two broad peaks at 140 and 127 ppm aforementioned, two other signal peaks at 150.0 and 120.9 ppm can be ascribed to part of substituted and unsubstituted phenyl carbons of spirobifluorenes, respectively. In addition, the signal peak of quaternary carbons in spirobifluorenes is also observed at 67.1 ppm. As for TPOP-4 and TPOP-5 prepared by oxidative coupling polymerization, their ^{13}C CP/MAS NMR spectra are shown in Fig. S2† with similar signal distribution.

The porosity and porous structure of the polymers were studied by sorption analysis using nitrogen as the sorbate molecule. Typical nitrogen adsorption–desorption isotherms of these polymers are shown in Fig. 2 and S3†. According to the physisorption isotherms measured at 77 K, all polymers are microporous and show a combination of type I and II nitrogen gas sorption isotherms according to the IUPAC classification.[22] The isotherms display a continuous increase after the adsorption at low relative pressure, indicating an adsorption on the outer surface of small particles. The increase in the nitrogen uptake at a high relative pressure above 0.9 could be explained by condensation of nitrogen in the meso- and macrostructures of the samples and interparticular voids, respectively.[12b] In addition, hysteresis was observed for the whole range of relative pressure based on the isotherms, which is attributed to the swelling in a flexible polymer framework or the restricted access of adsorbate to pores blocked by narrow openings, especially for non-ordered nanoporous materials.[12b,23]

Listed in Table 1 are the key structural properties derived from the isotherm, such as BET and Langmuir surface areas, micropore surface areas and volumes. The BET specific surface areas for these polymers range from 472 m^2 g^{-1} (TPOP-1) to 810 m^2 g^{-1} (TPOP-5), which are calculated over the relative pressure (P/P_0) range from 0.01 to 0.1 according to the previous report, which gives a better fit than using the relative pressure range of 0.05–0.2 (see Fig. S5–9 and Table S1†).[24] It should be noted that when tetrakis(4-bromophenyl) ethylene (**M-1**) was used as the only one core structural monomer, the obtained homopolymer (TPOP-1) shows a low BET specific surface area. Similar result was found for homopolymer **P1** (450 m^2 g^{-1}) obtained using the same

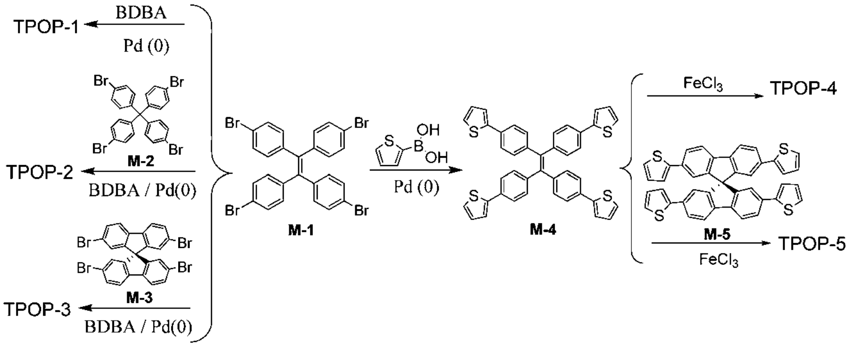

Scheme 1 Preparation of TPOPs by Suzuki coupling polymerization and oxidative coupling polymerization.

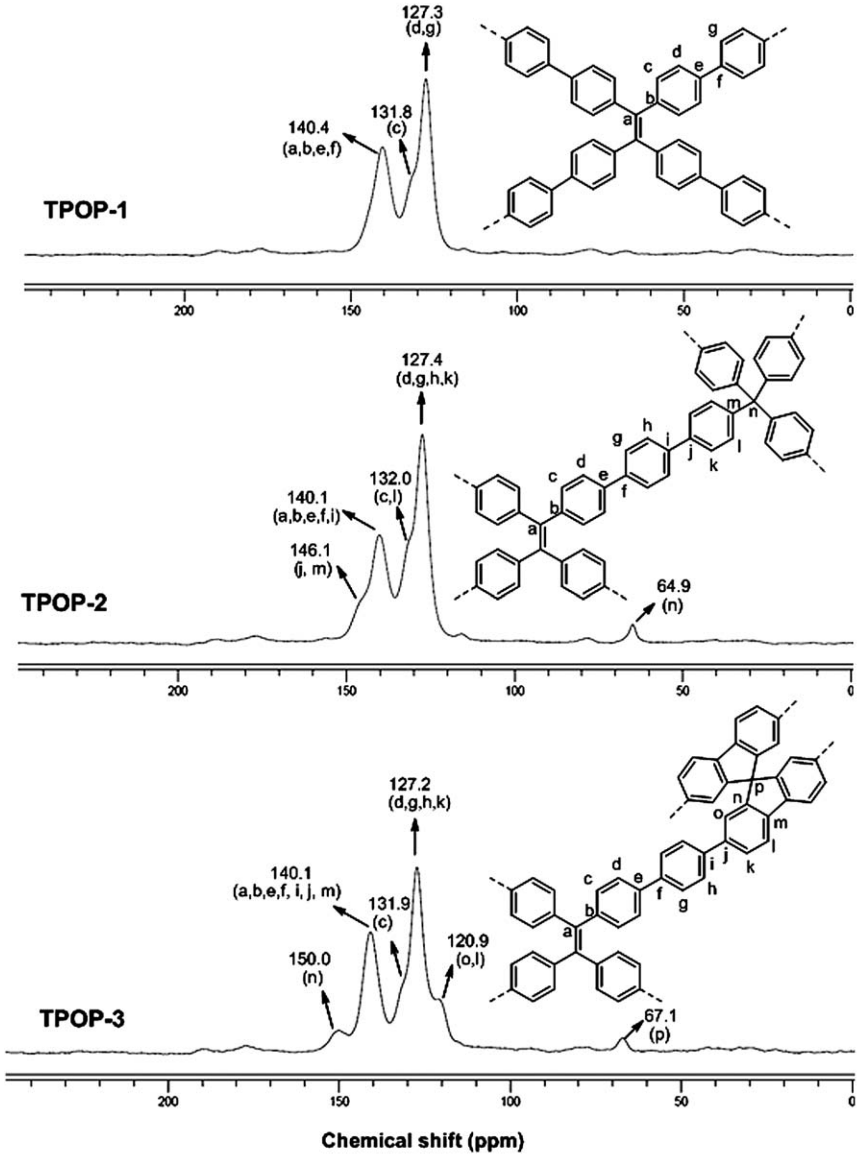

Fig. 1 Selected ^{13}C CP/MAS NMR spectra of prepared TPOPs.

method by Weber and Thomas,[11a] in which only tetrabromospirobifluorene (**M-3**) is a core structural monomer. However, when the same amount of **M-1** and **M-3** were used as core constructing monomers together, the BET specific surface area of the synthetic copolymer (TPOP-3) increases to 765 m^2 g^{-1}. When **M-3** was replaced by tetrakis(4-bromophenyl) methane (**M-2**), another copolymer (TPOP-2) can be obtained through the same procedure, and its BET specific surface area is 673 m^2 g^{-1}, which is also higher than that of TPOP-1. Using the method of oxidative coupling of thiophenes, synthetic polymer TPOP-5 containing two different core structural monomers possesses a higher BET specific surface area (810 m^2 g^{-1}) than TPOP-4 (681 m^2 g^{-1}). Cooper's group[6b] has reported preparation and physisorption properties of poly(aryleneethynylene) (PAE) homopolymers and copolymers. Using a same core structural building block, the micropore size and surface area of PAE polymers can be fine-tuned by systematic variation of the monomer strut length. Additionally, both the BET specific surface area and the Langmuir surface area of the series of copolymers fall between the related homopolymers. In light of some cases in our work, keeping the length of the linker monomer (BDBA) same, the surface area of copolymers prepared by two different core structural monomers is higher than that of the corresponding homopolymers. These results might provide some new clues for the design and synthesis of porous organic polymers.

For the non-ordered porous materials, accurate determination of the pore size distribution (PSD) is very difficult. Different results are usually obtained according to different calculation methods. Furthermore, the pronounced hysteresis indicates that porous polymers are swelling during the nitrogen sorption measurement, which suggests that the pore structure probably changes during the measurement. PSD analysis based on the NLDFT approach has been used extensively to characterize a wide variety of similar porous materials, although it does have limitations.[12a,24b] However, the calculated results can give some

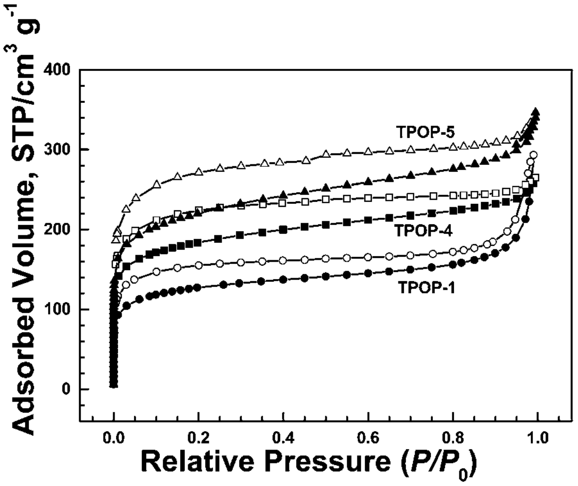

Fig. 2 Nitrogen adsorption–desorption isotherms of TPOPs measured at 77 K. (The adsorption and desorption branches are labeled with filled and open symbols, respectively.) See the ESI for a logarithmic plot of adsorption isotherms (Fig. S4†).

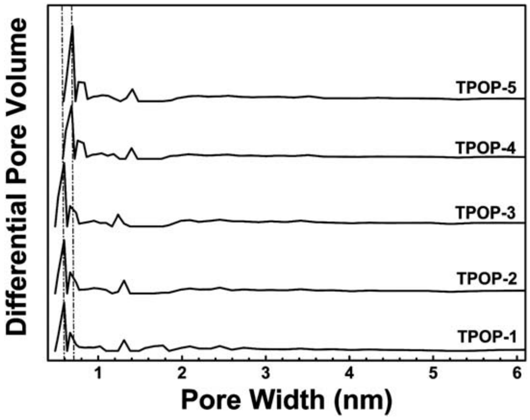

Fig. 3 Pore size distribution of TPOPs calculated by the NLDFT approach.

related qualitative information, with which one can make a relative comparison of materials synthesized from different monomers. The PSDs of TPOPs were calculated from the NLDFT approach. As shown in Fig. 3, for TPOPs prepared by the Suzuki coupling polycondensation, pore widths are mainly centered at 0.58 nm. Meanwhile, polymers TPOP-4 and TPOP-5 exhibit a similar pore size distribution with a dominant pore width at 0.67 nm. Fig. S4† indicates that there is no big difference in the nitrogen uptake behavior of TPOPs at the low relative pressure (P/P_0 < 0.1). On account of the good capacity in hydrogen adsorption for many porous materials, we investigated their hydrogen uptake based on the hydrogen physisorption isotherms measured at 77 K up to a pressure of 1.13 bar (Fig. 4). An increase in the total hydrogen capacity with increasing surface area is observed. TPOP-5, possessing the highest micropore volume and highest BET specific surface area, exhibits the largest hydrogen uptake of 1.07 wt% at 1.13 bar and 77 K. The hydrogen uptake capacity of TPOP-5 is not only higher than some previously obtained porous organic polymers with similar surface areas[14,25] but also comparable to the reported element organic framework, EOF-7, with a higher BET specific surface area (1.14 wt% at 1 bar and 77 K, S_{BET} = 1083 m^2 g^{-1}).[12b] As shown in Fig. S10†, the hydrogen uptake behaviors of TPOPs are similar at the low pressure range (P < 100 mmHg). From the hydrogen physisorption isotherms, we can see that TPOP-1 and TPOP-2 seem to follow a linear increasing uptake at higher pressures, while the others are inclined to level off. This suggests that, as the randomly packed networks, conformation changes of some polymers have probably taken place with enhancing pressure, due to rotation and stretching of the building units, which may provide some "hidden" micropores and surface area in the polymers for hydrogen to continually permeate into these materials.

As expected, all TPE-based nanoporous organic polymers show a non-ordered, amorphous structure proved by the X-ray diffraction (XRD) measurements, due to the kinetic control of the polymerization. Fig. 5 and S11† show the scanning electron microscopy images and high-resolution transmission electron microscopy images of the obtained polymers, respectively. They exhibit a similar morphology with different particle sizes. The typical SEM images of TPOP-3 (Fig. 5a and b) indicate that the polymer consists of relatively uniform solid submicrometre spheres with particle sizes from 100 to 150 nm. Whereas the particle sizes of spheres in TPOP-4 are generally above 200 nm (Fig. 5d and e). Small macropores or mesopores in the polymers can be ascribed mostly to the interparticulate porosity that exists between agglomerated microgel particles.[26] The TEM images (Fig. 5c and f) are indicative of porous structures of the materials, which are similar to some reported amorphous microporous organic polymers.[6a]

As aforementioned, TPE-based luminophor possesses the AIE features. In the aggregate form or solid state, its

Table 1 Porosities and hydrogen uptake capacities of TPOPs

TPOPs	Monomer(s)	S_{BET}[a]/m^2 g^{-1}	S_{micro}[b]/m^2 g^{-1}	V_{total}[c]/cm^3 g^{-1}	V_{micro}[d]/cm^3 g^{-1}	Hydrogen uptake[e] (wt%)
TPOP-1	**M-1**	472 (533)	297	0.330	0.119	0.83
TPOP-2	**M-1** + **M-2**	673 (760)	368	0.462	0.150	0.91
TPOP-3	**M-1** + **M-3**	765 (851)	369	0.491	0.153	1.00
TPOP-4	**M-4**	681 (768)	422	0.380	0.170	0.96
TPOP-5	**M-4** + **M-5**	810 (912)	445	0.479	0.181	1.07

[a] Specific surface area calculated from the nitrogen adsorption isotherm using the BET method. The number in parentheses is the Langmuir surface area calculated from the nitrogen adsorption isotherm by application of the Langmuir equation. [b] Micropore surface area calculated from the nitrogen adsorption isotherm using the *t*-plot method. [c] Total pore volume at P/P_0 = 0.97. [d] Micropore volume derived using the *t*-plot method based on the Halsey thickness equation. [e] Data were obtained at 1.13 bar and 77 K.

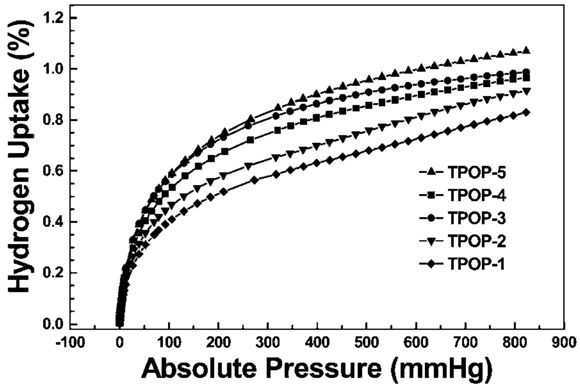

Fig. 4 Gravimetric hydrogen adsorption isotherms for TPOP-1 (diamonds), TPOP-2 (down triangles), TPOP-3 (circles), TPOP-4 (squares), and TPOP-5 (up triangles) at 77 K. See the ESI for a logarithmic plot of adsorption isotherms (Fig. S10†).

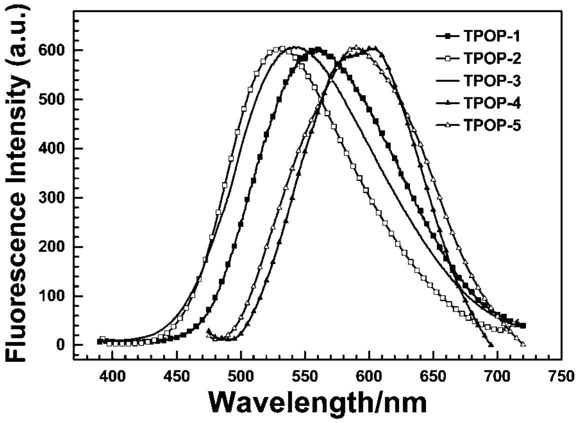

Fig. 6 Fluorescent spectra of the polymers in the solid state (excitation wavelength is 365 nm).

photoluminescence intensity can be greatly enhanced. Because of the network structure of the prepared porous polymers, intramolecular rotations of the TPE moieties are restricted. Therefore, we can expect that TPE-based porous polymers shall exhibit strong photoluminescence properties. Fig. 6 summarizes the fluorescent properties of the polymers. Based on the emission spectra, the maximum peaks of all polymers range from 530 to 610 nm, which are assigned to the π–π^* transition of the conjugated backbone. TPOP-3 exhibits an emission maximum peak at 540 nm in the solid state. Compared with TPOP-3, the blue shift in emission is observed for TPOP-2 which shows an emission maximum peak at 530 nm (green emission, Fig. 6), probably ascribed to the decreased extent of π-orbital overlap owing to the tetraphenylmethane moieties. Furthermore, compared to copolymers TPOP-2 and TPOP-3, polymer TPOP-1 displays an emission maximum peak at 560 nm (yellow emission, Fig. 6). The red shift could be owing to the relatively enhanced planar conformation of polymer backbone for TPOP-1 in the solid state, considering that two different contorted core structural monomers are used to construct the network structure of TPOP-2 and TPOP-3. Moreover, due to the electron-rich thiophene moieties with efficient charge carrier transport property, the polymers of TPOP-4 and TPOP-5 show emission maximum peaks at 590 and 610 nm, respectively. Photos of selected polymers under UV light (365 nm) illumination are shown in Fig. S12†. Weber and Thomas have also reported the emission spectrum of the similar spirobifluorene-based polymer **P1** with a maximum peak at 460 nm (blue emission).[11a] Based on our studies, the photoluminescence properties of porous polymers can be tuned significantly by substituting a half amount of spirobifluorene building blocks with tetraphenylethylene, which implies that the optical properties of the porous organic polymers can also be controlled by using proper constructing monomers.

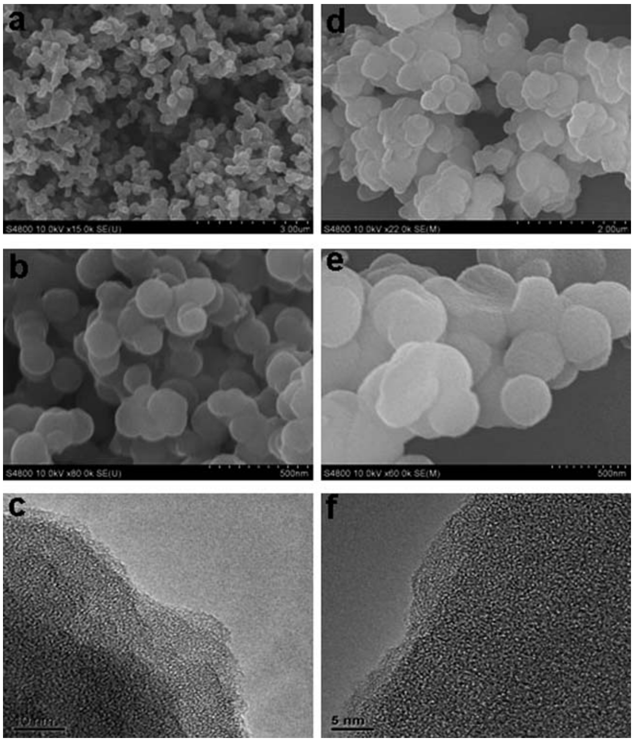

Fig. 5 SEM images of TPOP-3 (a and b) and TPOP-4 (d and e) and TEM images of TPOP-3 (c) and TPOP-4 (f).

4. Conclusion

TPE-based porous organic polymers were prepared successfully through palladium-catalyzed Suzuki coupling polymerization and oxidative coupling polymerization, respectively. BET specific surface areas for these polymers vary between 472 and 810 $m^2\ g^{-1}$, based on different core structural building blocks. Incorporation of tetraphenylethylene moieties into these polymers induced high photoluminescence (λ_{max}: 530–610 nm) in the solid state. Because of the propeller-like structure and AIE characteristics, tetraphenylethylene is proved to be a novel building block for the design of porous polymers with special properties. Different types of contorted or non-planar core structures with similar reactivity would have great impact on the gas sorption and photoluminescence properties of polymers. By selecting proper building units, both surface area and optical property of porous organic polymers can be fine-tuned.

Acknowledgements

The financial supports of the Ministry of Science and Technology of China (Grant 2011CB932502), National Science Foundation of China (Grants 20972035, 91023001, and 21002017), and the Chinese Academy of Science (Grant KJCX2-YW-H21) are acknowledged.

References

1 (*a*) L. Chen, Y. Yang and D. Jiang, *J. Am. Chem. Soc.*, 2010, **132**, 9138–9143; (*b*) X. Du, Y. Sun, B. Tan, Q. Teng, X. Yao, C. Su and W. Wang, *Chem. Commun.*, 2010, **46**, 970–972.

2 (*a*) C. J. Doonan, D. J. Tranchemontagne, T. G. Glover, J. R. Hunt and O. M. Yaghi, *Nat. Chem.*, 2010, **2**, 235–238; (*b*) J. H. Choi, K. M. Choi, H. J. Jeon, Y. J. Choi, Y. Lee and J. K. Kang, *Macromolecules*, 2010, **43**, 5508–5511.

3 (*a*) J. H. Ahn, J. E. Jang, C. G. Oh, S. K. Ihm, J. Cortez and D. C. Sherrington, *Macromolecules*, 2006, **39**, 627–632; (*b*) C. D. Wood, B. Tan, A. Trewin, F. Su, M. J. Rosseinsky, D. Bradshaw, Y. Sun, L. Zhou and A. I. Cooper, *Adv. Mater.*, 2008, **20**, 1916–1920; (*c*) J. Germain, J. M. J. Frechét and F. Svec, *Chem. Commun.*, 2009, 1526–1528; (*d*) F. Svec, J. Germain and J. M. J. Frechét, *Small*, 2009, **5**, 1098–1111.

4 (*a*) N. B. McKeown and P. M. Budd, *Chem. Soc. Rev.*, 2006, **35**, 675–683; (*b*) N. B. McKeown and P. M. Budd, *Macromolecules*, 2010, **43**, 5163–5176.

5 (*a*) H. M. El-Kaderi, J. R. Hunt, J. L. Mendoza-Cortés, A. P. Côté, R. E. Taylor, M. O'Keeffe and O. M. Yaghi, *Science*, 2007, **316**, 268–272; (*b*) A. P. Côté, A. I. Benin, N. W. Ockwig, M. O'Keeffe, A. J. Matzger and O. M. Yaghi, *Science*, 2005, **310**, 1166–1170.

6 (*a*) J. X. Jiang, F. Su, A. Trewin, C. D. Wood, N. L. Campbell, H. Niu, C. Dickinson, A. Y. Ganin, M. J. Rosseinsky, Y. Z. Khimyak and A. I. Cooper, *Angew. Chem., Int. Ed.*, 2007, **46**, 8574–8578; (*b*) J. X. Jiang, F. Su, A. Trewin, C. D. Wood, H. Niu, J. T. A. Jones, Y. Z. Khimyak and A. I. Cooper, *J. Am. Chem. Soc.*, 2008, **130**, 7710–7720; (*c*) A. I. Cooper, *Adv. Mater.*, 2009, **21**, 1291–1295.

7 S. Yuan, B. Dorney, D. White, S. Kirklin, P. Zapol, L. Yu and D.-J. Liu, *Chem. Commun.*, 2010, **46**, 4547–4549.

8 (*a*) S. Yuan, S. Kirklin, B. Dorney, D.-J. Liu and L. Yu, *Macromolecules*, 2009, **42**, 1554–1559; (*b*) J. Schmidt, J. Weber, J. D. Epping, M. Antonietti and A. Thormas, *Adv. Mater.*, 2009, **21**, 702–705.

9 (*a*) J. Schmidt, M. Werner and A. Thomas, *Macromolecules*, 2009, **42**, 4426–4429; (*b*) T. Ben, H. Rao, S. Ma, D. Cao, J. Lan, X. Jing, W. Wang, J. Xu, F. Deng, J. M. Simmons, S. Qui and G. Zhu, *Angew. Chem., Int. Ed.*, 2009, **48**, 9457–9460.

10 (*a*) P. Kuhn, A. Forget, D. S. Su, A. Thomas and M. Antonietti, *J. Am. Chem. Soc.*, 2008, **130**, 13333–13337; (*b*) P. Kuhn, A. Thomas and M. Antonietti, *Macromolecules*, 2009, **42**, 319–326.

11 (*a*) J. Weber and A. Thomas, *J. Am. Chem. Soc.*, 2008, **130**, 6334–6335; (*b*) J. Weber, M. Antonietti and A. Thomas, *Macromolecules*, 2008, **41**, 2880–2885.

12 (*a*) E. Stöckel, X. Wu, A. Trewin, C. D. Wood, R. Clowes, N. L. Campbell, J. T. A. Jones, Y. Z. Khimyak, D. J. Adams and A. I. Cooper, *Chem. Commun.*, 2009, 212–214; (*b*) M. Rose, N. Klein, W. Böhlmann, B. Böhringer, S. Fichtner and S. Kaskel, *Soft Matter*, 2010, **6**, 3918–3923.

13 W. Chaikittisilp, A. Sugawara, A. Shimojima and T. Okubo, *Chem.–Eur. J.*, 2010, **16**, 6006–6014.

14 H. Lim and J. Y. Chang, *Macromolecules*, 2010, **43**, 6943–6945.

15 Y. Dong, J. W. Y. Lam, A. Qin, J. Liu, Z. Li, B. Z. Tang, J. Sun and H. S. Kwok, *Appl. Phys. Lett.*, 2007, **91**, 011111.

16 (*a*) A. Qin, J. W. Y. Lam, L. Tang, C. K. W. Jim, H. Zhao, J. Sun and B. Z. Tang, *Macromolecules*, 2009, **42**, 1421–1424; (*b*) L. Liu, G. Zhang, J. Xiang, D. Zhang and D. Zhu, *Org. Lett.*, 2008, **10**, 4581–4584; (*c*) X.-M. Hu, Q. Chen, D. Zhou, J. Cao, Y.-J. He and B.-H. Han, *Polym. Chem.*, 2011, **2**, 1124–1128.

17 (*a*) H. Tong, Y. N. Hong, Y. Q. Dong, M. Haussler, Z. Li, J. W. Y. Lam, Y. P. Dong, H. H. Y. Sung, I. D. Williams and B. Z. Tang, *J. Phys. Chem. B*, 2007, **111**, 11817–11823; (*b*) Y. Hong, M. Haussler, J. W. Y. Lam, Z. Li, K. K. Sin, Y. Dong, H. Tong, J. Liu, A. Qin, R. Renneberg and B. Z. Tang, *Chem.–Eur. J.*, 2008, **14**, 6428–6437; (*c*) M. Wang, X. Gu, G. Zhang, D. Zhang and D. Zhu, *Anal. Chem.*, 2009, **81**, 4444–4449; (*d*) L. Peng, G. Zhang, D. Zhang, J. Xiang, R. Zhao, Y. Wang and D. Zhu, *Org. Lett.*, 2009, **11**, 4014–4017; (*e*) T. Kato, A. Kawaguchi, K. Nagata and K. Hatanaka, *Biochem. Biophys. Res. Commun.*, 2010, **394**, 200–204; (*f*) Q. Chen, N. Bian, C. Cao, X.-L. Qiu, A.-D. Qi and B.-H. Han, *Chem. Commun.*, 2010, **46**, 4067–4069; (*g*) J.-X. Wang, Q. Chen, N. Bian, F. Yang, J. Sun, A.-D. Qi, C.-G. Yan and B.-H. Han, *Org. Biomol. Chem.*, 2011, **9**, 2219–2226.

18 X.-F. Duan, J. Zeng, J.-W. Lv and Z.-B. Zhang, *J. Org. Chem.*, 2006, **71**, 9873–9876.

19 R. L. Wu, J. S. Schumm, D. L. Pearson and J. M. Tour, *J. Org. Chem.*, 1996, **61**, 6906–6921.

20 M. Grimm, B. Hirste and H. Hurrock, *Angew. Chem., Int. Ed. Engl.*, 1986, **25**, 1097–1098.

21 J.-X. Jiang, A. Trewin, F. Su, C. D. Wood, H. Niu, J. T. A. Jones, Y. Z. Khimyak and A. I. Cooper, *Macromolecules*, 2009, **42**, 2658–2666.

22 K. S. W. Sing, D. H. Everett, R. A. W. Haul, L. Moscou, R. A. Pierotti, J. Rouquérol and T. Siemieniewska, *Pure Appl. Chem.*, 1985, **57**, 603–619.

23 M. Rose, W. Böhlmann, M. Sabo and S. Kaskel, *Chem. Commun.*, 2008, 2462–2464.

24 (*a*) K. S. Walton and R. Q. Snurr, *J. Am. Chem. Soc.*, 2007, **129**, 8552–8556; (*b*) J. Weber, J. Schmidt, A. Thomas and W. Böhlmann, *Langmuir*, 2010, **26**, 15650–15656.

25 R. Dawson, F. Su, H. Niu, C. D. Wood, J. T. A. Jones, Y. Z. Khimyak and A. I. Cooper, *Macromolecules*, 2008, **41**, 1591–1593.

26 J.-X. Jiang, F. Su, H. Niu, C. D. Wood, N. L. Campbell, Y. Z. Khimyak and A. I. Cooper, *Chem. Commun.*, 2008, 486–488.